European Research Infrastructure supporting Smart Grid Systems Technology Development, Validation and Roll Out

.

Technical Report TA User Project

To Investigate the Impact of Cumulative Penetration of PV Systems into the Distribution Network

Grant Agreement No:	**654113**
Funding Instrument:	**Research and Innovation Actions (RIA) – Integrating Activity (IA)**
Funded under:	**INFRAIA-1-2014/2015: Integrating and opening existing national and regional research infrastructures of European interest**
Starting date of project:	**01.11.2015**
Project Duration:	**54 months**

Delivery date:	**30.04.2020**
Name of lead beneficiary for this deliverable:	**Arvind Sharma, University of Agder, Norway**
Deliverable Type:	**Report (R)**
Security Class:	**Public**
Revision / Status:	**Released**

Project co-funded by the European Commission within the H2020 Programme (2014-2020)

Document Information

Document Version:	2
Revision / Status:	Released
All Authors/Partners	Arvind Sharma, University of Agder Alkistis Kontou, ICCS-NTUA
Distribution List	Public

Document History

Revision	Content / Changes	Resp. Partner	Date
1	Draft document ready for review	Arvind Sharma	17/03/2020
2	Final version	Arvind Sharma, Alkistis Kontou	30/04/2020

Document Approval

Final Approval	Name	Resp. Partner	Date
Review and improvements	Alkistis Kontou,	ICCS-NTUA	15/04/2020

Disclaimer

Copyright Notice

Table of Contents

Abbreviations

BESS	Battery Energy Storage System
DER	Distributed Energy Resource
DG	Distributed Generator
DRTS	Digital Real-Time Simulator
ESS	Energy Storage System
ICT	Information and Communication Technology
MV/LV	Medium Voltage/Low voltage
P	Active Power
PCC	Point of Common Coupling
PHIL	Power Hardware in the Loop
PV	Photovoltaic
Q	Reactive Power
RES	Renewable Energy Source
RTDS	Real-Time Digital Simulator
NTUA	National Technical University of Athens

Executive Summary

This Transnational Access project investigated voltage rise issues due to the high PV penetration in MV networks and their mitigation by implementing the droop control concept in PV inverters. The main contribution of this research is to investigate the impact of inverters when participating in the reactive power control within specific types of MV distribution networks. In detail, this work investigates this solution when inverters are operating in grid-tied mode and experiments are performed using a digital real time simulator (DRTS). A hardware PV inverter and a simulated battery energy storage system were operated in parallel, using real-time simulation and the Power Hardware in-Loop (PHIL) method. The experimental results justify the usefulness of using inverters as means of reactive power control in the MV grid. In this work, different grid topologies (e.g. connecting feeders) are created and tested, and the results are analysed to assess the high PV penetration impacts for the different grid topologies.

1 General Information of the User Project

The general information of the user project is shown as below.

User Project Title: To Investigate the Impact of High PV Penetration into the Medium Voltage Distributed Network

User Project Acronym: PV Systems

Host Infrastructure: ICCS-NTUA

Start date - End date: 12/01/2020 to 01/02/2020

User Group Member: Arvind Sharma, PhD Research Fellow, University of Agder, Norway

2 Research Motivation

Distributed power system network with solar photovoltaic system is becoming very popular in all over the world. In several European countries and regions e.g. Germany, Spain, Belgium and others, several distribution networks (e.g. low voltage - LV network) have reached high PV penetration levels [1]. Traditionally, medium/low voltage distribution networks possess unbalanced characteristics due to the unbalanced line configurations and phase loadings. Also, these networks have not been designed for multi-direction power flows. Nevertheless, with the integration of solar PV systems into the distributed network, MV network is going to become active with effective customers participation. It is going to impact the power flows within network power as well as power quality. Consequently, the utility operators, with existing information will face difficulties in getting control over the distribution network performance and operation.

The major impacts of PV integration have been observed as voltage variations and unbalance, harmonics, power quality issues, protection circuits etc [2]. Rapid variations in the solar irradiation can also cause voltage fluctuations/flicker issues and the incidences may exacerbate in the network, if the PV penetration is going to increase [3]. In the existing system most of the solar PV systems are connected as injecting the power into the network without giving effective contribution for managing the voltage, and power flows [4]. Most of these issues can be resolved through designing and implementing innovative control strategy within the distributed network.

Integration of distributed energy sources via intelligent power conditioning devices within the distributed network can help in managing the power flows as well as improving the power quality. The power conditioning devices are required to operate intelligently considering available synthetic inertia within the distributed network for managing the system stability and control under dynamic conditions within the distributed network.

Based on the above-mentioned key issues / challenges, two main research areas are investigated in this work. First area of research has investigated the impact of penetration of PV systems into the distributed network using digital real time simulator (DRTS) that includes multi-directional power flow (active and reactive) analysis and operational analysis within the distributed network at different solar radiation as well as loading conditions. In the second area of research area, a Hardware-In-Loop method used for testing of a real hardware PV inverter and Q(V) droop control strategy is implemented to address the voltage rise issues.

2.1 Objectives

The goal of this work is to analyse above mentioned issues / challenges related to high PV penetration and implement the Q-V droop control strategy to mitigate voltage fluctuation problems. Following are the key objectives of the proposed work

- Analyze the impact of high PV penetration using DRTS system into the different buses within the in medium voltage network and implement the droop control to mitigate the voltage fluctuation problem.
- Design and develop Power Hardware-in-Loop (PHIL) configurations to test a hardware PV inverter and implement the droop characteristics to address the voltage fluctuation problems.

2.2 Scope

The report explains the scenarios that are tested in the lab which includes the theoretical explanation and the results. In the entire sets of experiment, droop control technique is employed to realize optimum reactive power management via PV inverters in a medium voltage network.

Droop is a popular control technique usually explored to supply voltage regulation services where users can configure the inverter to generate ancillary services based on set limit applied to reactive power (Q_{min} and Q_{max}) and the voltage, ensuring the inverter can work at its maximum rating if required.

The droop technique has been verified in the experiments through PHIL setup having PV inverters in a MV grid. In order to analyse the test results, different parameters are recorded e.g. voltage at bus terminals, line loading, transformer loading, active and reactive power of the inverter and power flow at each bus terminal. In this work a typical CIGRE medium voltage (MV) network is selected.

3 State-of-the-Art/State-of-Technology

As the concerns for environmental pollution caused by fossil fuels keep rising and the energy policies sustain improvement, the renewable energy penetration is increasing rapidly. Among several distributed generation technologies, solar PV system is one of the fastest growing technology worldwide due to decreasing capital costs and technological advancements [5-8]. PV technology is being promoted through numerous ways e.g. centralized PV power plant, grid-connected PV rooftop, off-grid PV systems, micro-grid etc.

In a very recent development under EcoGrid EU project coordinated by SINTEF and was carried out on Bornholm – a Danish island connected to the Nordic electricity market. The project aims to develop modern information and communication technology (ICT) and innovative market solutions to use more than 50% renewable energy sources (RES) remove the barriers that currently prevent small-scale consumers from participating in the power-balancing market [9]. In [10], Younicos in close collaboration with the Azorean power utility EDA, established a megawatt-scale grid-forming renewable energy system for Graciosa island in Portugal. Intelligent power controls and energy management system are combined with a 4 MW/3.2 MWh battery storage system powered by lithium-ion battery, a 4.5 MW wind park and a 1 MW photovoltaic power plant. The “island mode” capability of the fully automated battery system will enable up to 100 percent spontaneous renewable power penetration and allow the Portuguese island to replace around two-thirds of its fossil fuel generation with cheap renewable energy.

In many European countries and regions e.g. Germany, Spain, Belgium and others, several LV grids have reached high PV penetration levels. This may cause severe problems on the distribution network due to intermittent nature and uncontrolled dispatch of power from the PV systems [11]. Traditionally, low voltage distribution networks possess unbalanced characteristics due to the unbalanced line configurations and phase loadings. Also, these networks are not designed for two-way power flows. Nevertheless, with the distributed integration of solar PV systems into the grid, the distributed network(s) are becoming active, and the customers can export and import power to the grid, which could impact the power management as well as voltage profile. Consequently, the utility operators, with existing information will face difficulties in getting control over the distribution network performance and operation especially in case on high penetration of distributed PV systems. There are many challenges for increasing the penetration of PV into distributed network and it will raise operational and control difficulties as well as maintaining the power quality and stability within the micro-grid [12, 13].

The major impacts of PV integration have been observed as voltage variations, unbalanced loads, harmonics, power quality issues, protection relays etc [14]. Rapid variations in the solar irradiation can also cause voltage fluctuations/flicker issues and such incidences may exacerbate in the network if the PV penetration increases [15]. In Germany, to overcome over-voltage events, from January 2012, a fixed limitation of the active power (i.e. 70% of the nominal peak-output power of the PV system) feed-in by each PV system has become mandatory [16]. Some other alternative solutions to curtailment of active power by domestic load shifting, to increase local consumption, and energy storage are discussed in ref [17]. The application of battery storage with the PV system has also been studied [18] and most of the studies are focusing on load management rather than controllable dispatching of the power within the distributed network [19].

Based on the above-mentioned key issues / challenges it is significantly important to investigate and analyse the potential issues with high PV system penetration in the existing distribution networks and implement the mitigation techniques which can be useful to address these challenges.

4 Executed Tests and Experiments

In this work, two main experiments are conducted using DRTS and PHIL method. The section below

provides general picture of the test beds, plan and parameters considered for the setup and procedure for executing the test.

4.1 Test Plan

1) Experiment 1 – In the experiment 1, impacts of high PV penetration are studied in the CIGRE MV network using DRTS system, and droop control techniques are implemented to address the voltage rise problems.
2) Experiment 2 – The impacts of PV system penetration are analysed using PHIL method, and Q(V) droop control strategy is implemented in the real hardware PV inverter to address the voltage rise problems.

In the experiment no 1, DRTS system and RSCAD software are used for analyzing the impacts of PV system penetration into the distribution network however, in the experiment no. 2 hardware in-loop method is used in which real hardware PV inverter is connected with the DRTS. The DRTS system available at ICCS-NTUA, Athens as shown in Fig. 1a and testing setup using PHIL method as shown in Fig. 1b.

a)

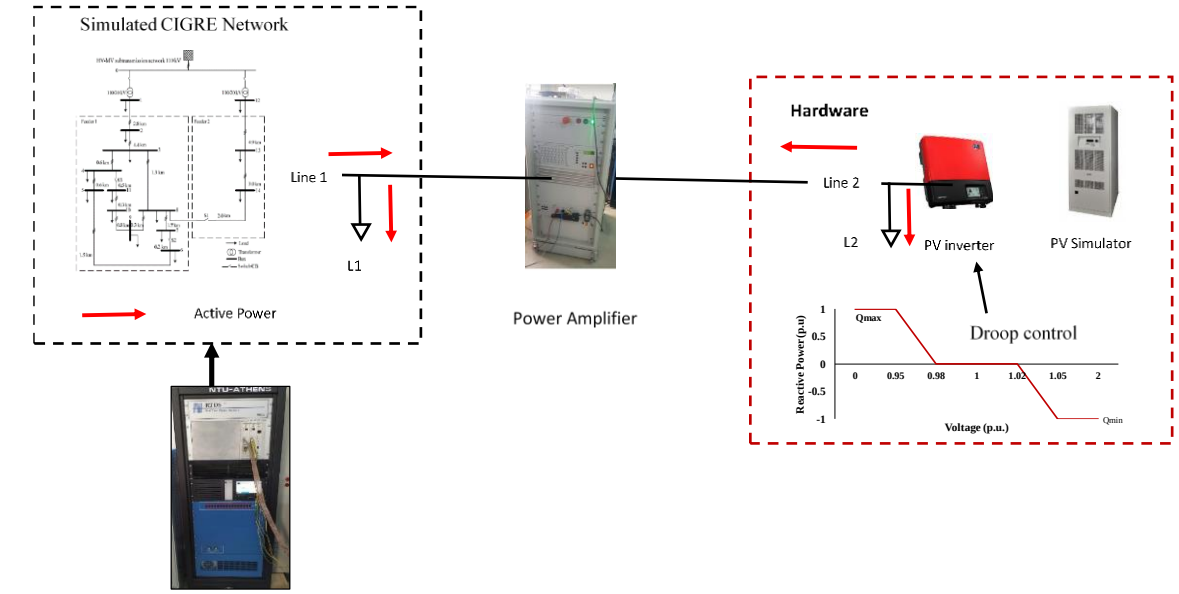

b)

DRTS

Fig. 1: Test setup of the PHIL experiment
a) Real Time Digital Simulator and amplifier at ICCS-NTUA, Athens
b) Diagram of the PHIL test setup

4.2 Standards, Procedures, and Methodology

In order to conduct the experiments, below mentioned steps are followed

1) Designing of selected distribution network circuit in the RSCAD and, test and run the different operational scenarios.
2) Check the simulation result to ensure there shouldn't be any hazard for the hardware that will be connected.
3) Connect the hardware devices to the RTDS and conduct experiment.
4) Test and measure the voltage, line loading and transformer loadings.
5) Test and measure the reactive power compensation established from the droop-controlled inverter and its response time.
6) Test and measure the active power generated by all PV inverter.
7) Examine the contribution of the inverter to local loads.
8) Create different grid topologies by closing Switches S_1, S_2 and S_3. More details about the selected MV grid topology is given in the next section.
9) Obtain and save the results from the RT simulation using MATLAB.

5 Experiment 1

The selected topology of the MV distribution network has shown in the Fig. 2. The electrical network consists of Feeders 1 and 2, and these are connected separately with two winding transformers (rated 25 MVA at 110kV/20kV), TR_1 and TR_2 respectively. The network consists of 14 buses and three switches (i.e. S_1, S_2 and S_3) which can be used to create a radial or mesh type electrical network. In experiment 1, switches S_1, S_2 and S_3 are kept open and network behaves like a pure radial network. The buses B_1 and B_{12} are the reference buses in the distribution network. The buses B_2 to B_{11} are connected to the feeder 1 however, Buses B_{13} and B_{14} are connected to the Feeder 2. The technical details of transformers, cables such as line length, voltage & current rating, resistance, inductance, load type and power factor are given in the ref [20]. The considered MV distribution network is modelled in the RSCAD software and used to analyze the results with DRTS system.

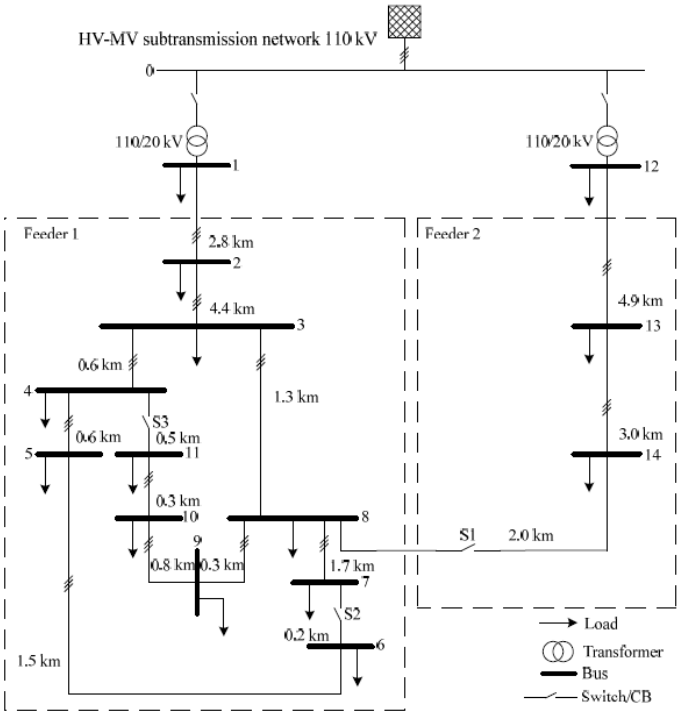

Fig. 2 Topology of CIGRE MV distribution network benchmark

5.1 EXP1 - System and Test Description

In the Experiment 1, bus B_8 is selected for investing the impact of high PV penetration into the electrical distribution network. In this experiment, three cases are investigated; in the Case 1.1, PV system is not connected to the MV network, and bus voltages and other parameters (i.e. line loading, transformer loading) are measured however, in the Case 1.2, PV system is connected to bus B_8 and the measurements of the second experiment are compared with those of Case 1.1. The voltage rise issue observed in the Case 1.2 and mitigated by implementing Q(V) droop control in the PV inverter in the Case 1.3.

The reactive power -voltage *Q(U)* droop control corrects voltage errors in the network by injecting or

absorbing reactive power as a result of changes to the nominal voltage. PV inverter's response depends on the configured parameters of the droop controller, i.e. the voltage dead-bands, Q_{min} and Q_{max}, the gain, as shown in Fig. 3. The application of the Droop Control concept is investigated in order to improve the voltage profiles so that more PV could be connected to the MV distribution network. With the application of the Q(V) droop control, inverter can positively contribute to feeder's voltage control and can result in an improved voltage profile. The design of the inverter controller's response must be very fast in terms of responding to changes in the MV network.

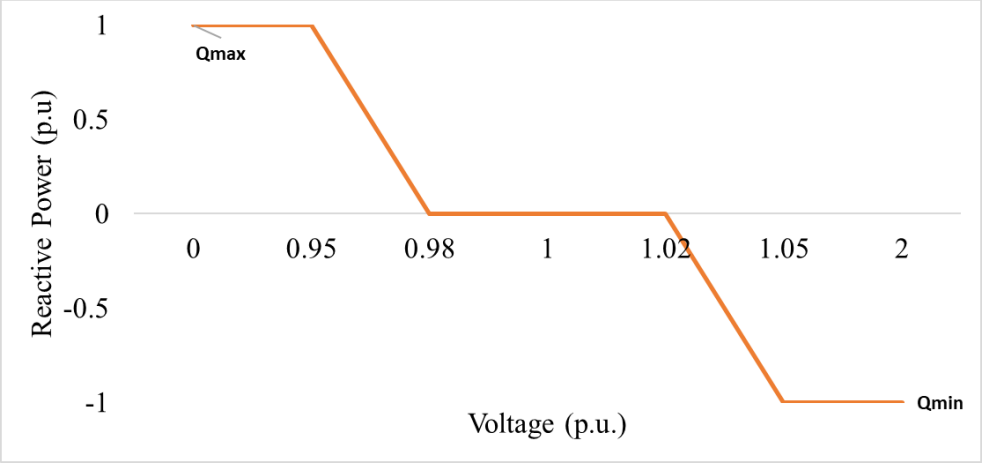

Fig. 3: The inverter's Voltage Droop Control

A Q(V) droop controller is designed for the PV system in order to mitigate voltage deviations, by injecting or absorbing reactive power. The block diagram of the control system in RSCAD has shown in the Fig. 4. The voltage of bus B_8, is monitored and used as an input parameter for the droop controller. The characteristic curve of the Q(V) droop controller is shown in Fig. 3, based on which the Q_{droop} of the PV inverter is generated. The gain (droop) of the used controller is 33.33 and as it is calculated from the slope of the Q(V) graph. In addition, the design of the control system takes into consideration the maximum apparent power of the PV inverter, in order every moment the active and reactive power components not to exceed inverter's capability. Last, the switch DRen is placed in order to activate and deactivate the Q(V) control.

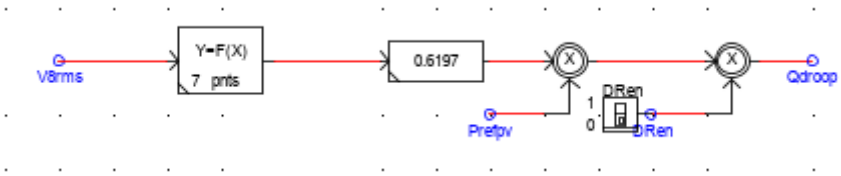

Fig. 4: Modelling of the inverter's Voltage Droop Control

5.2 EXP1 - Test Setup

The Novacor real time digital simulator (RTDS) is used for conducting the experiment no. 1 and is illustrated in the Fig.1a.

5.3 Results and Discussion

5.3.1 EXP1.1 – PV system is not connected to the MV network

As explained in the previous section, Case 1.1 analysed the results of base case scenario when PV is not connected to the MV network. There are total 14 buses within the selected MV network, in which buses B_2 to B_{11} are connected to Feeder 1 and buses B_{13} and B_{14} to the Feeder 2. In order to compare and analyze the results of the experimental work, all 14 buses are categorised into three Groups A, B and C. Group A comprises buses B_1 to B_6, Group B comprises buses B_7 to B_{11} whereas Group C comprises buses B_{12} to B_{14}. Similarly, corresponding lines are also categorised in Group A, B and C. Lines L_1L_2, L_2L_3, L_3L_4, L_4L_5 and L_5L_6 are under Group A, Lines L_7L_8, L_8L_9, L_9L_{10}, $L_{10}L_{11}$ and L_3L_8 are in Group B, Lines $L_{12}L_{13}$, and $L_{13}L_{14}$ in the Group C.

Table 1: Active and reactive power at different buses in the MV network

Bus no.	Active Power (MW)	Reactive Power (MVA)
Bus 1	12.44	2.96
Bus 2	0	0
Bus 3	0.27	0.12
Bus 4	0.22	0.05
Bus 5	0.36	0.09
Bus 6	0.27	0.07
Bus 7	0.07	0.04
Bus 8	0.47	0.12
Bus 9	0.59	0.15
Bus 10	0.44	0.13
Bus 11	0.26	0.07
Bus 12	11.56	3.17
Bus 13	0.03	0.02
Bus 14	5	1.73

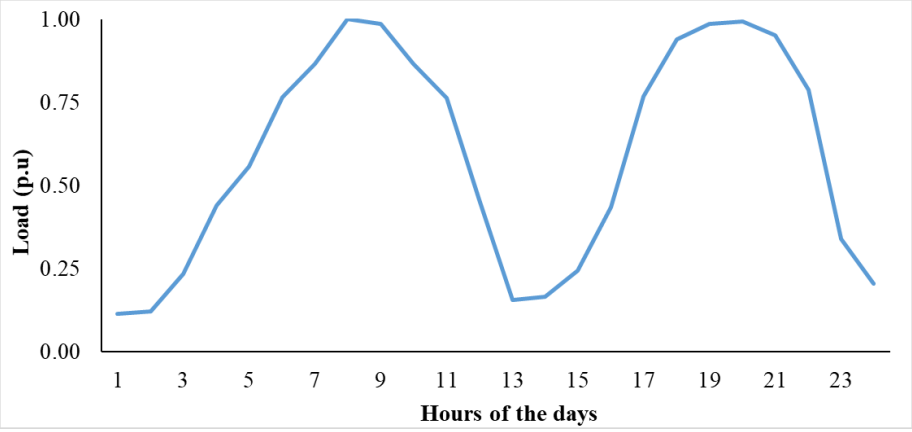

Fig. 5: Typical load profile of the selected MV Network

A typical daily load profile is used to evaluate the performance of MV distribution network, and its illustration has shown in the Fig. 5. In order to generate a typical daily load profile, slider is used in the RSCAD and output of the slider is given to the corresponding loads connected with different buses however, maximum load demands (i.e. active and reactive power) are varied for different buses and their values are given in Table 1. In the base case scenario (i.e. Case 1.1) the maximum load demand at different buses are chosen so that it would not violate the bus voltage regulation (i.e. $0.90 \leq V_i \leq 1.10$ p.u.), line loading and transformer loading (e.g. 100%). It has been observed from the daily load profile that the minimum load demand is 0.12 p. u. and it appeared during the night-time (00:00 hours to 01:00 hours) and daytime (11:00 hours to 14:00 hours). The demand increased to 1 p. u. in the morning (08:00 hours 09:00 hours) and night (20:00 hours 21:00 hours).

Group A of Case 1.1: In Group A, voltage (p. u.) of six buses (i.e. B_1 to B_6), loading (%) of five lines (i.e. L_1L_2, L_2L_3, L_3L_4, L_4L_5 and L_5L_6) are shown in the Figs. 6 & 7. The bus voltage of all six buses (i.e. V_1 to V_6) never goes below 0.94 p.u. and raised up to 1.0 p.u. The lowest voltages are appeared during the peak demand's hours of 08:00 hours to 09:00 hours and 20:00 hours to 21:00 hours. The maximum line loading is recorded 18% for the lines L_1L_2 and L_2L_3, whereas, loadings of the remaining lines (i.e. L_3L_4, L_4L_5 and L_5L_6) are remains below 5% throughout the day.

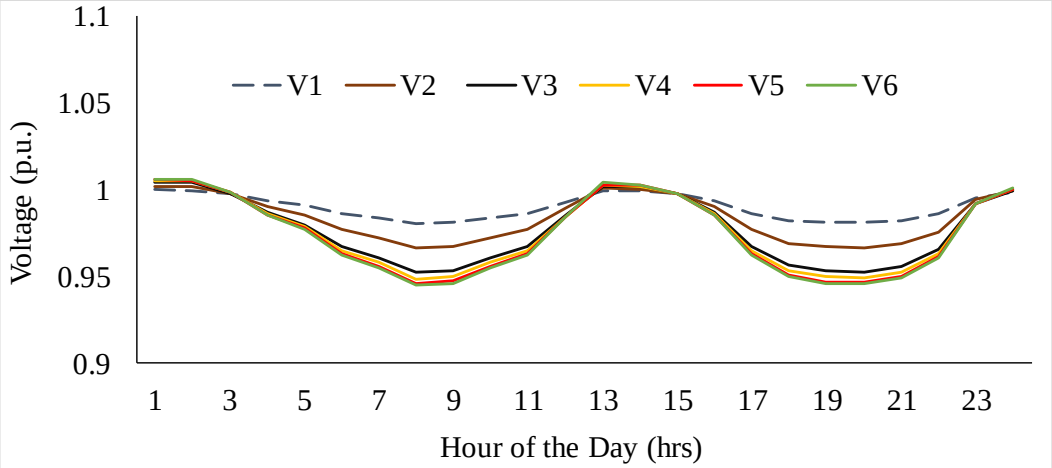

Fig. 6: Variation of bus voltages in a typical day

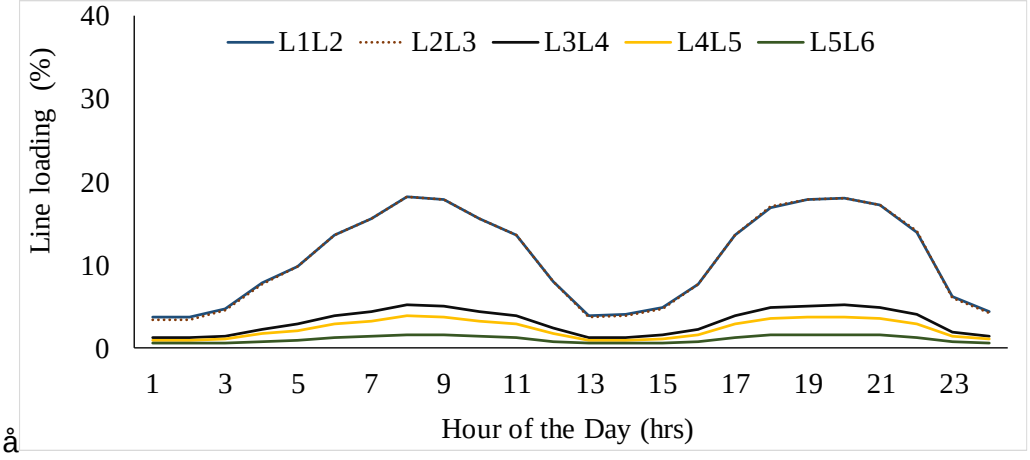

Fig. 7: Variation of line loading in a typical day

Group B of Case 1.1: In the Group B, voltage (p. u.) of five buses (i.e. B_7 to B_{11}), loading (%) of five Lines (i.e. 7-8, 8-9, 9-10,10-11 and 3-8) and have shown in the Figs. 8 & 9. The bus voltage of all

six buses (i.e. V_1 to V_6) never goes below than 0.93 p.u. The lowest voltage is appeared during the peak demand's hours of 08:00 hrs. to 09:00 hrs. and 20:00 hrs. to 21:00 hrs. The maximum line loading has been recorded 12% for the lines 1-2 and 2-3, whereas, loadings of the remaining lines (i.e. L_7L_8, L_8L_9, L_9L_{10}, $L_{10}L_{11}$ and L_3L_8) are remains below 10% throughout the day.

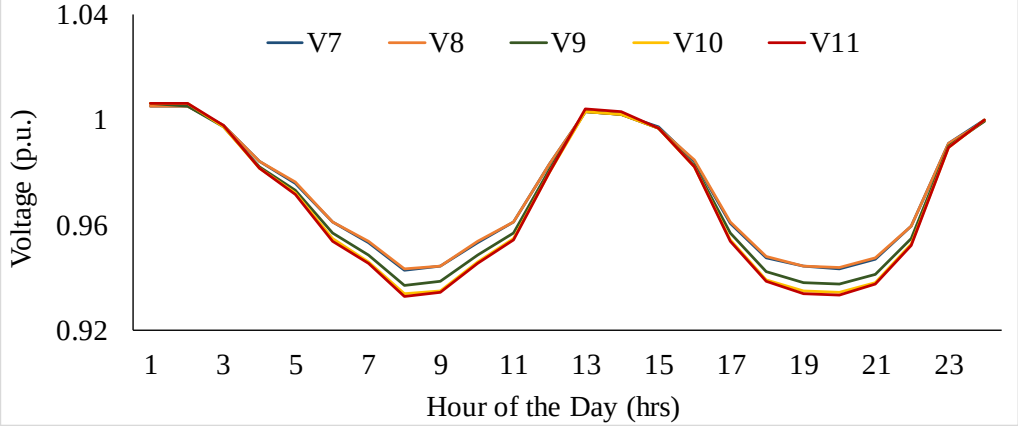

Fig. 8: Variation of bus voltages in a typical day

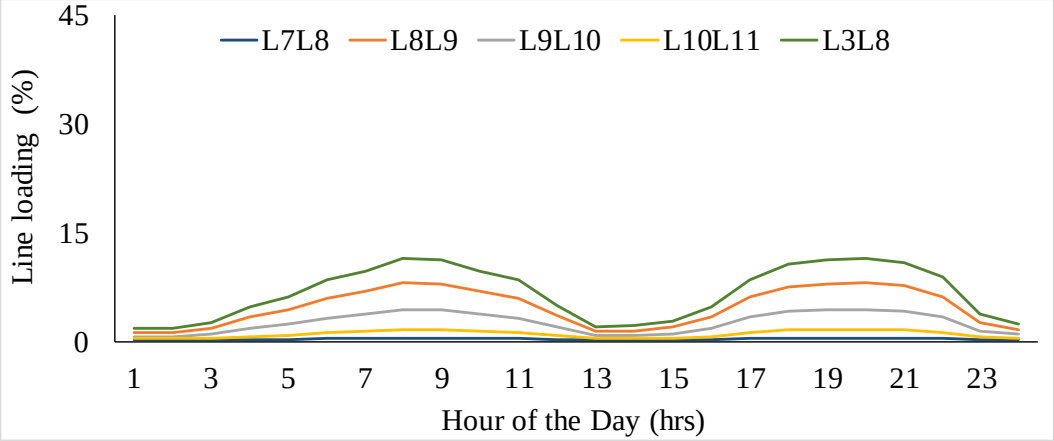

Fig. 9: Variation of line loadings in a typical day

Group C of Case 1.1: In the Group C, voltage (p. u.) of three buses (B_{12} to B_{14}), loading (%) of two lines (i.e. $L_{12}L_{13}$ and $L_{13}L_{14}$) and are shown in the Figs. 10 &11. The bus voltage of two buses (i.e. V_{13} and V_{14}) never goes below than 0.92 p.u. The lowest voltage is appeared during the peak demand's hours of 08:00 hrs. to 09:00 hrs. and 20:00 hrs. to 21:00 hrs. The maximum line loading is recorded 44% for the lines $L_{12}L_{13}$ and $L_{13}L_{14}$. Since, there is no PV connected to the feeder 2 therefore voltage and line loading are not affected in the feeder 2. During the maximum load demand the maximum loading of transformer TL_1 and TL_2 are observed 63% and 76% respectively. In the next section (i.e. Case 1.2) 15 MW capacity of PV system is connected to the bus B_8 and results are discussed.

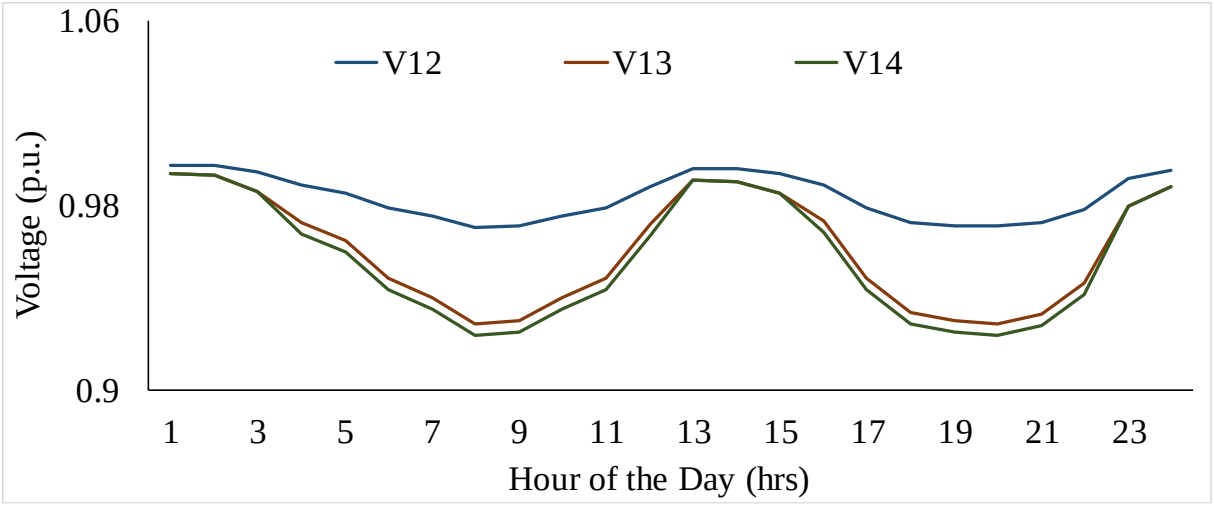

Fig. 10: Variation of bus voltages in a typical day

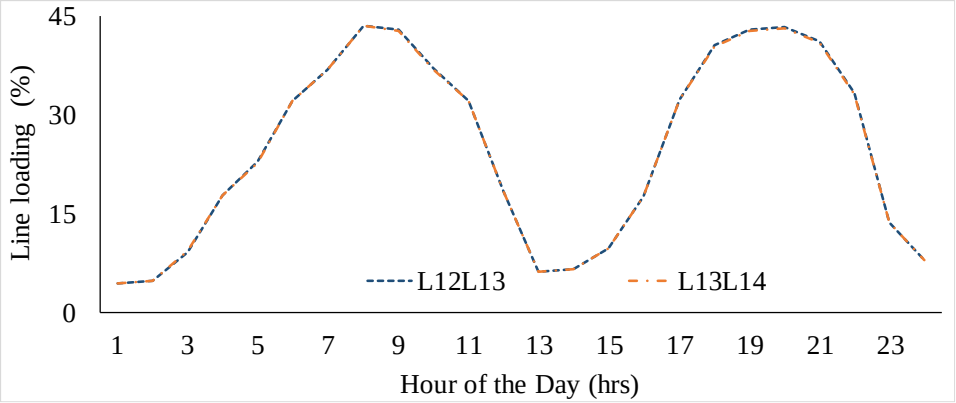

Fig. 11: Variation of line loadings in a typical day

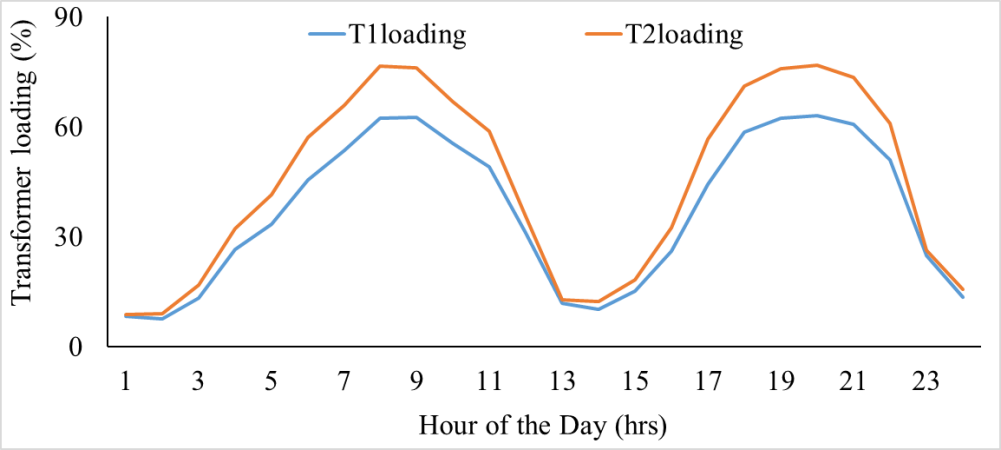

Fig. 12: Variation of transformers loading in a typical day

5.3.2 EXP 1.2: 15 MW PV system connected at bus 8, without Q(V) droop control

Group A of Case 1.2: In this case, a PV of 15 MW capacity is connected to bus B_8 and voltage and

line loadings are observed. The variation of solar PV output for typical day is shown in Fig. 13. The maximum solar PV output of 1 p.u (15 MW) is appeared at 13:00 hours. In Group A, voltage (p. u.) of six buses (i.e. B_1 to B_6), loading (%) of five lines (i.e. L_1L_2, L_2L_3, L_3L_4, L_4L_5 and L_5L_6) are shown in Figs. 14 &15 respectively. The bus voltage of all six buses (i.e. V_1 to V_6) never goes below than 0.94 p.u. however the maximum voltage is raised to 1.05 p.u. The maximum voltages are appeared during the peak sunshine hours at 13:00 hours. The maximum line loading is recorded 38% for the lines L_1L_2, and L_2L_3 whereas, loadings of the remaining lines (i.e. L_3L_4, L_4L_5 and L_5L_6) are remains below 5% throughout the day.

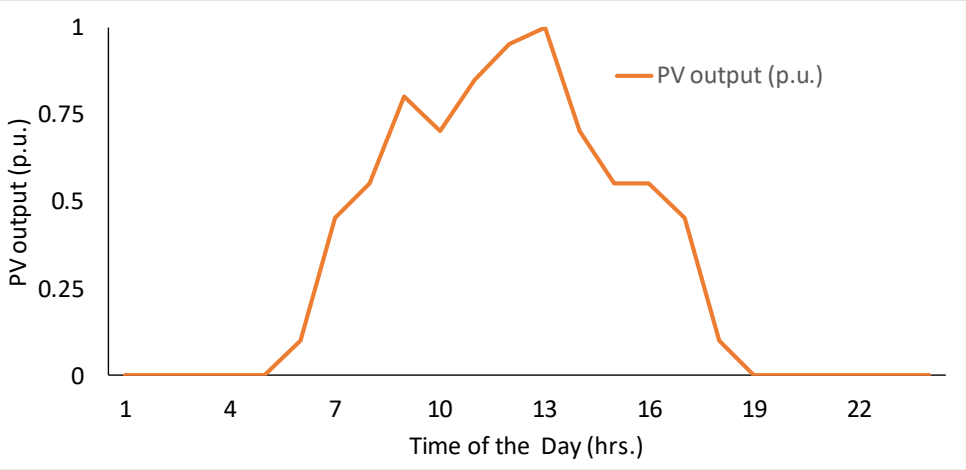

Fig. 13 Variation of PV output in a typical day

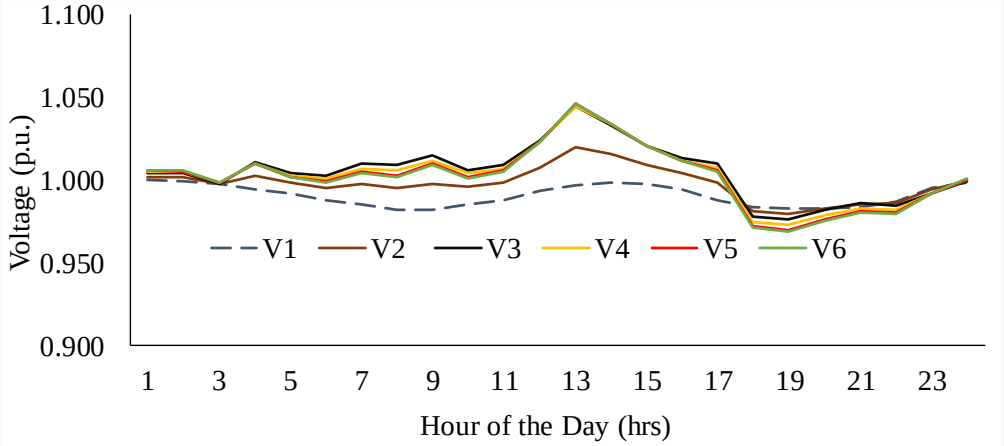

Fig. 14: Variation of bus voltages in a typical day

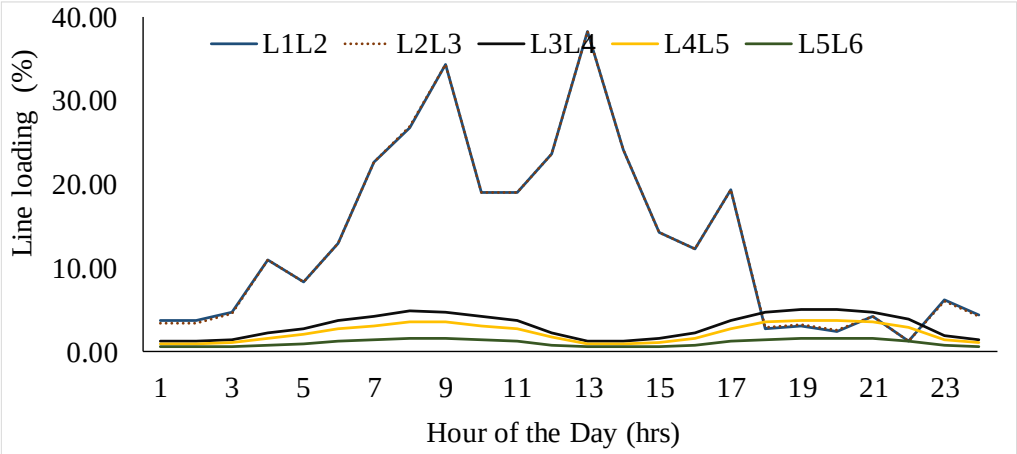

Fig. 15: Variation of line loadings in a typical day

By connecting 15 MW of solar PV system at bus number 8, significant rise in the bus voltages V_5, V_6 and V_7 are observed and further increase in the PV capacity can violate the high voltage limits.

Group B of Case 1.2: In the Group B, voltage (p. u.) of five buses (i.e. B_7 to B_{11}), loading (%) of five lines (i.e. L_7L_8, L_8L_9, L_9L_{10}, $L_{10}L_{11}$ and L_3L_8) are show in the Figs. 16 & 17 respectively. The bus voltage of all six buses (i.e. V_1 to V_6) never goes below than 0.93 p.u. but the maximum voltage is recorded 1.09 p.u. for buses B_8, B_9 and B_{10} during peak sunshine hours (i.e. 11:00 hours to 13:00 hours). The maximum loading of line 3-8 is recorded 43% whereas, loadings of the remaining lines (i.e. L_7L_8, L_8L_9, L_9L_{10}, and $L_{10}L_{11}$) are remains below 5% throughout the day.

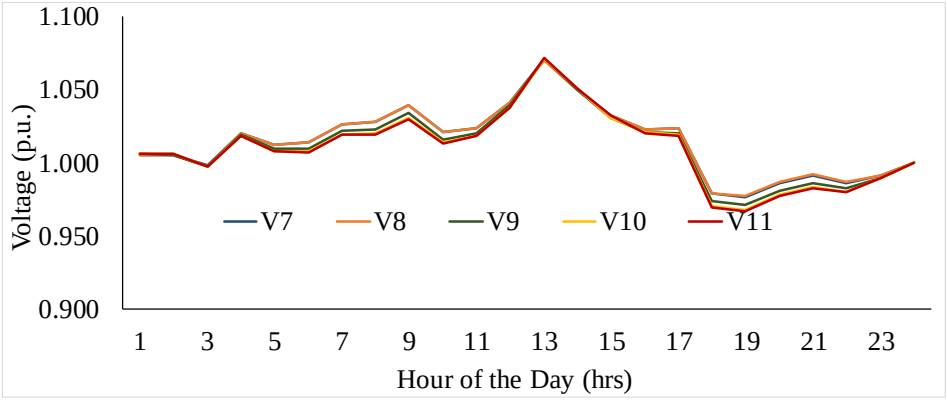

Fig. 16: Variation of bus voltages in a typical day

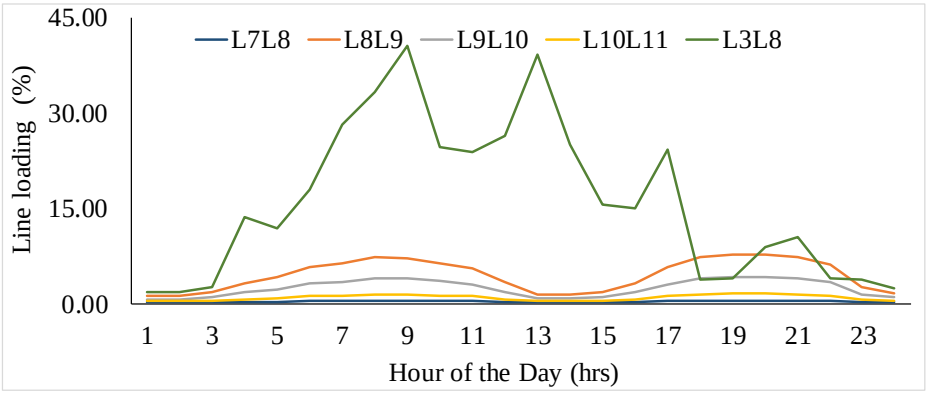

Fig. 17: Variation of line loadings in a typical day

In order to address the voltage-rise problem, Q(V) droop control strategy is implemented, and results are presented in the next section (i.e. Case 1.3).

5.3.3 EXP1.3 – 15 MW PV system connected at bus 8 with Q(V) droop control

In this experiment Q(V) droop control strategy is implemented and bus voltages and line loading are recorded and compared with the Case 1.2. The block diagram of the control system is shown in the Fig. 18. The more description about Q(V) droop control has given in the Section 5.1.

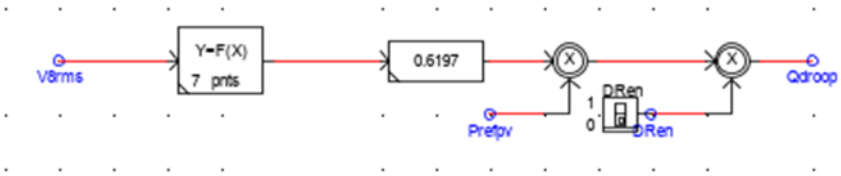

Fig. 18: The inverter's Voltage Droop Control

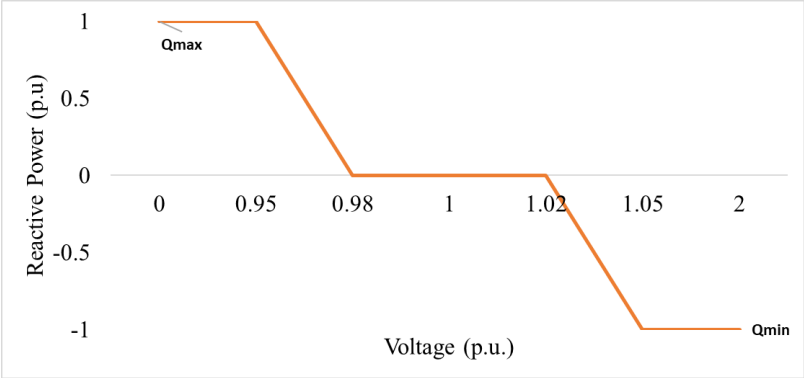

Fig. 19: The inverter's Voltage Droop Control

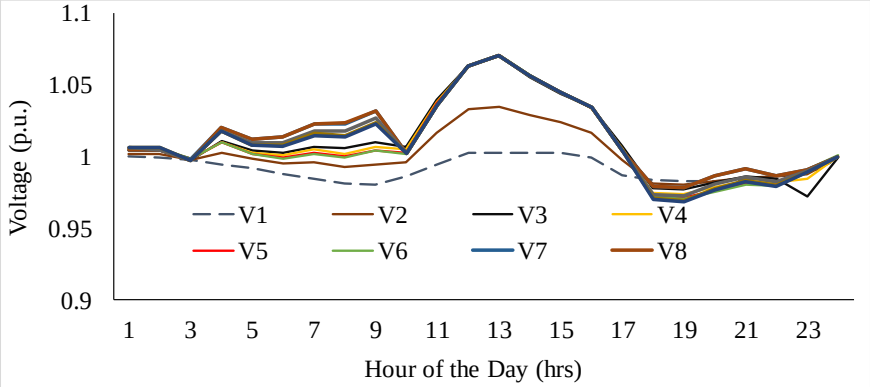

Fig. 20 Bus voltages at different bus terminals during a typical day

It has been observed from the Fig. 20 that the maximum voltage of buses B_8, B_9, B_{10} and B_{11} are improved significantly. As compare to the Case 1.2, the maximum voltage is reduced from 1.09 p.u. to 1.05. It also indicates that more PV can be connected within the distribution network. The line loadings of all the lines connected with feeder 1 are shown in the Fig. 21. As compare to the Case 1.2, line loading of line L_1L_2, L_2L_3 and L_3L_8 are increased from 15% to 42%. It happened because of 15 MW of PV is integration into the bus B_8.

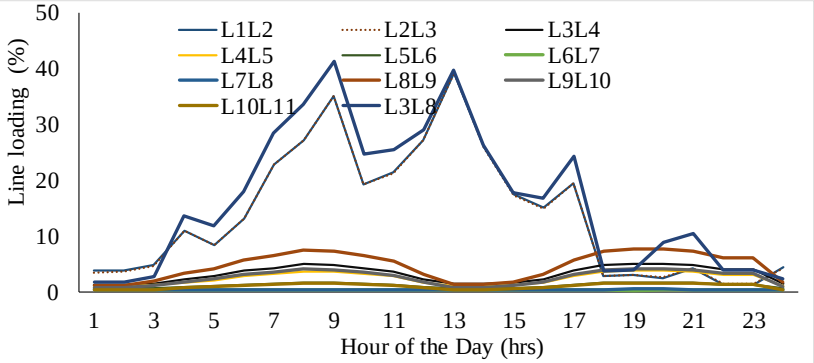

Fig. 21: Variation of Line loadings for a typical Day

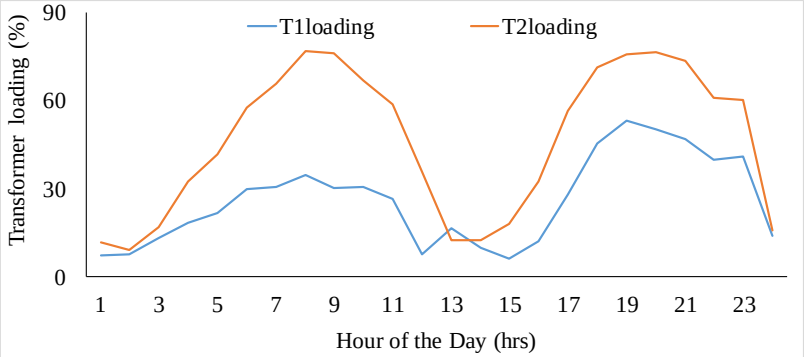

Fig. 22: Variation of transformer loadings for a typical Day

The loading of the transformers TL_1 and TL_2 are illustrated in the Fig 22. It has been observed from Fig. 22 that the maximum loading of transformer TL_1 is reduced to 53% from 63%, as extra PV generation is injected into the grid. However, loading characteristics of transformer TL_2 doesn't change and it follows the same characteristics as for Case 1.2. In this experiment PV is not connected into the feeder 2 and therefore, line loading, bus voltage and transformer loading are not changed.

6 Experiment 2

6.1 EXP2 - System and Test Description

This section investigates the dynamic functionality of a modelled droop-controlled inverter to address the high voltage problems into the selected MV network. The experiment is carried out using the PHIL test method combined with RTDS system, a hardware PV inverter, solar array simulator, power amplifier and a simulated MV electrical distribution network. The diagram of the test setup used in

this experiment is shown in the Fig. 23. Detail description about the PHIL method is given in the Section 4.1

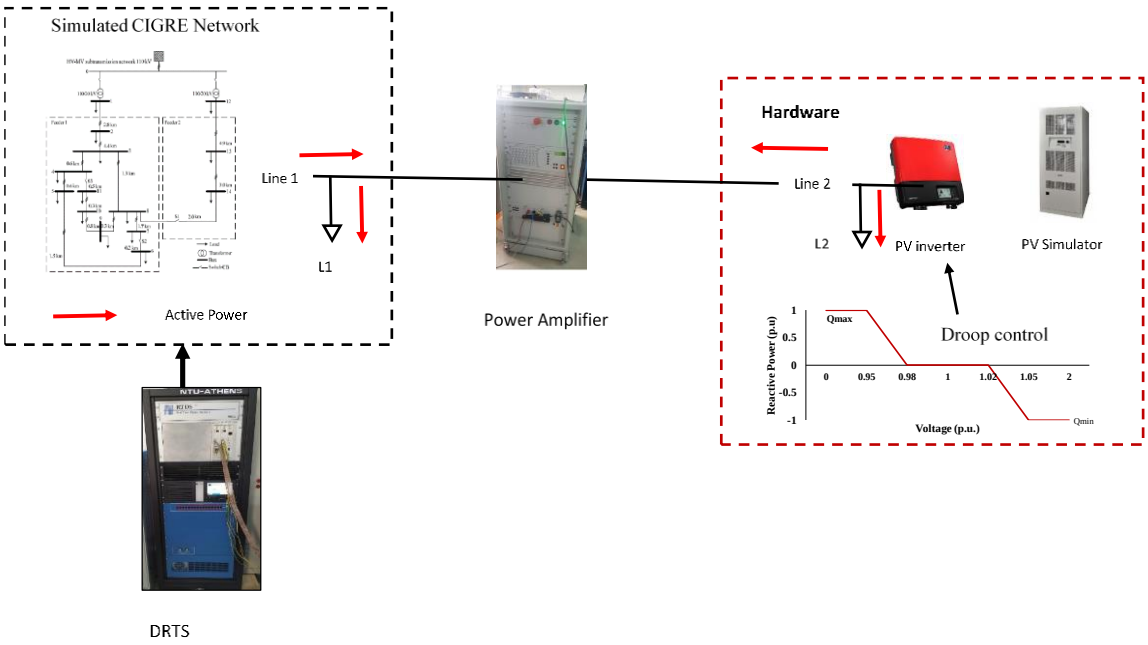

Fig. 23: PHIL testbed with hardware PV inverter using RTDS

6.2 EXP2 - Test Setup

The hardware PV inverter is connected on its DC side to a PV simulator, in order to allow fully controllable and customisable characteristics for the PV, such as maximum power point power, irradiance, temperature and so on. In addition, the hardware PV inverter communicates with a dedicated communication and control interfacing software, which enables the configuration of droop curve of the inverter. In the AC side, the PV inverter is connected with a linear power amplifier (Spitzenberger & Spies) which acts as an interface with the RTDS. Details about the connected PV system and their rating are given in the Table 2.

6.3 EXP2 – Test Results and Discussion

This experiment also analysed how the voltage rise issues are observed in different variations of grid topology. A summary of different tests carried out in this experiment are given in Table 2.

Table 2: Summary of the HIL tests used for the conducted experiments

Case No.	2 MVA PV at 7, 9,10 by RTDS	1MVA PV at bus 8 by HIL	Q(V) droop through HIL	Q(V) droop through RTDS	Switch position
Case 2.1	√	√	X	X	All open
Case 2.2	√	√	√	√	All open
Case 2.3	√	√	X	X	Only S3 closed
Case 2.4	√	√	√	√	Only S3 closed
Case 2.5	√	√	X	X	Only S2 closed
Case 2.6	√	√	√	√	Only S2 closed
Case 2.7	√	√	X	X	Only S1 closed
Case 2.8	√	√	√	√	Only S1 closed

6.3.1 Comparison of Test Cases 2.1 and 2.2

As stated in Table 2, 1 MVA of hardware PV inverter is connected at bus B_8 for conducting HIL experiment however, 2 MVA of simulated PV systems are connected to the bus B_7, B_9 and B_{10}. In addition to this, 1 MWh of simulated battery bank is integrated at bus B_8. In Case 2.1, PV systems are connected within the distribution network, but Q(V) droop control is not implemented however, in the Case 2.2, Q(V) droop control strategy is implemented. In this work, same droop control strategy is used (as discussed in the Case 1.3) for all PV systems. The changes in PV power output with time, connected to buses B_7, B_9 and B_{10} are shown in the Fig. 24. The variation of bus voltage in the buses of feeder 1 at different hours of the day for Case 2.1 and 2.2 are illustrated in Figs. 25 & 26 respectively. It has been observed that after implementing the Q(V) droop control, the maximum bus voltage of the Case 2.2. is decreased from 1.09 to 1.05 p.u.

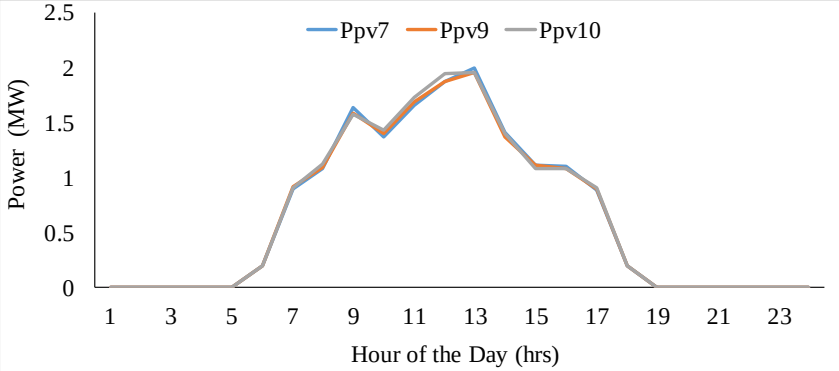

Fig. 24 Changes in PV power outputs at buses B_7, B_9 and B_{10}

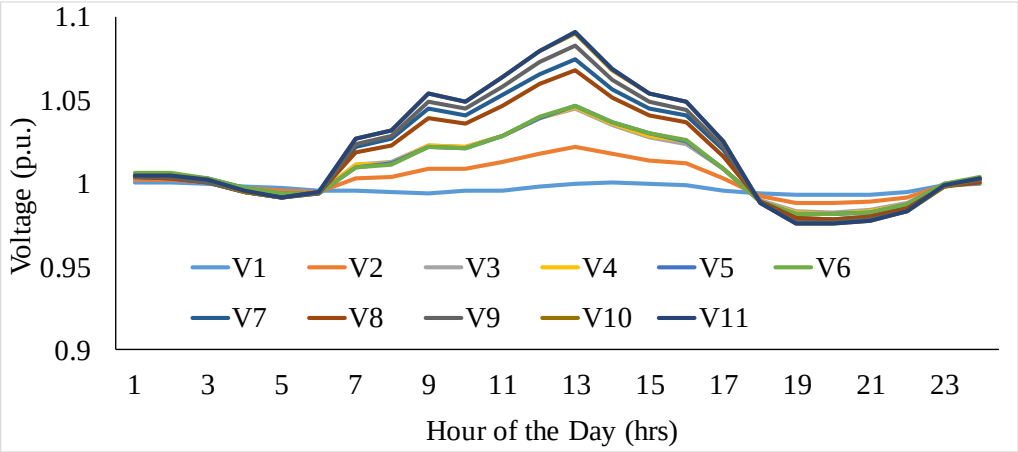

Fig. 25 Bus voltages at different bus terminals without Q(V) (Case 2.1)

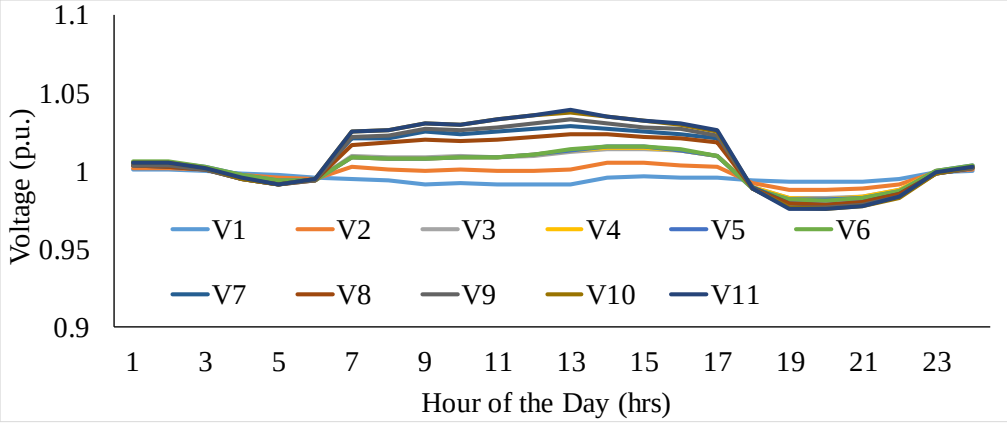

Fig. 26 Bus voltages at different bus terminals with Q(V) droop (Case 2.2)

The maximum PV power output of bus B_7, B_9 and B_{10} appeared 2 MW at 13:00 hours and shown in the Fig. 24. During the daytime (i.e. 8:00 hours to 17:00 hours) battery is getting charged whereas in the morning time (06:00 hours to 08:00 hours) battery is getting discharge. In the Fig. 27, battery discharging and changing are considered with positive (+) and negative signs respectively. It has been observed that PV inverter provide enough reactive power support (i.e. absorb) and reduce the bus voltage however there is no reactive power support from the battery. The maximum reactive power of 0.4 MVAr is absorbed by the inverter during 12:00 hours to 13:00 hours.

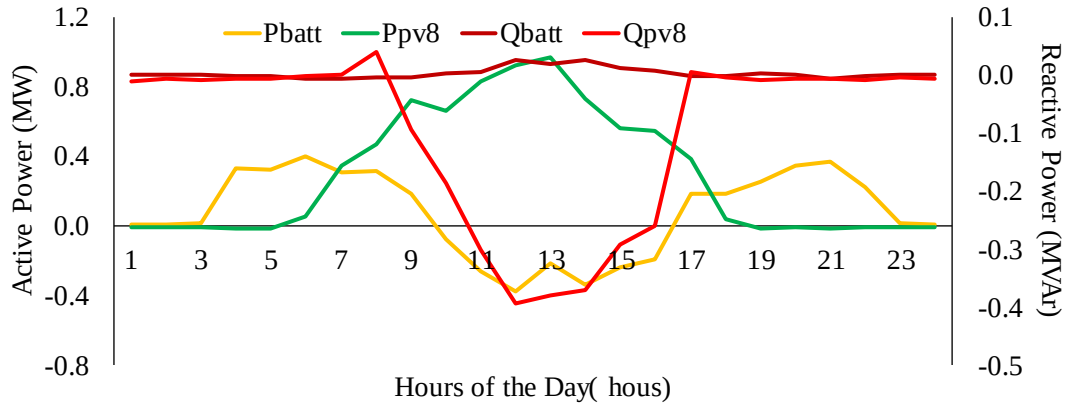

Fig. 27 Active and reactive power of PV and battery at bus terminal 8 (Case 2.2)

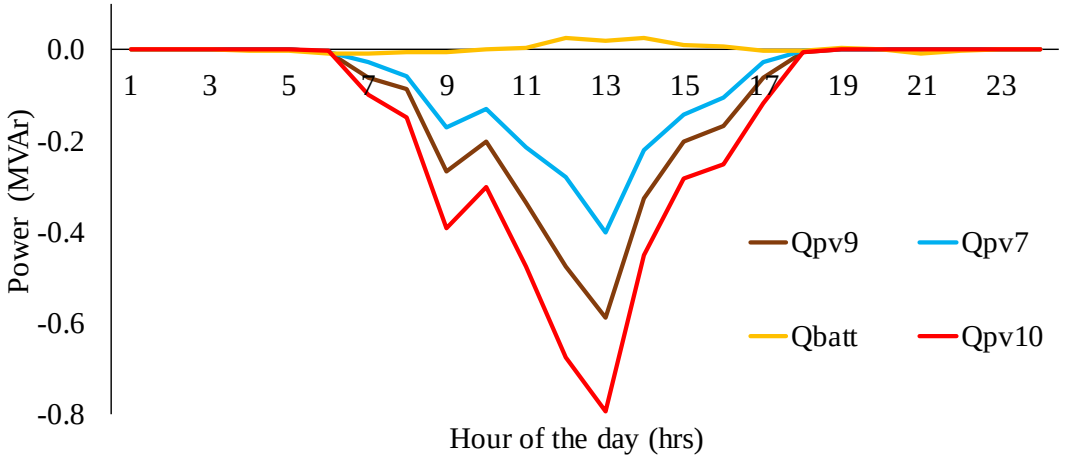

Fig. 28 Reactive power of PV inverter at bus B_7, B_8, and B_{10} (Case 2.2)

It has been observed from the Fig. 28 that PV inverter connected to bus B_{10} provides maximum reactive power support (i.e. absorbed) followed by PV inverter at bus B_9 and then PV inverter at bus B_7. This is because as maximum voltage rise appeared at bus B_{10} then followed by bus B_9 and then bus B_7 respectively. The variation of line loading and transformers loading are shown in the Figs. 29 and 30. It has been observed that line loading and transformer loadings in Case 2.1 and 2.2 are almost similar and there is no significant variation in both cases.

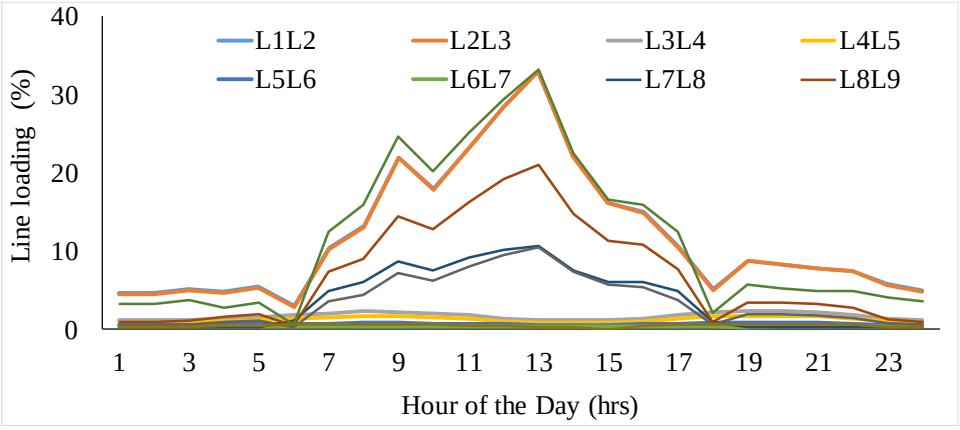

Fig. 29 Variation of Line loadings for a typical Day (Case 2.2)

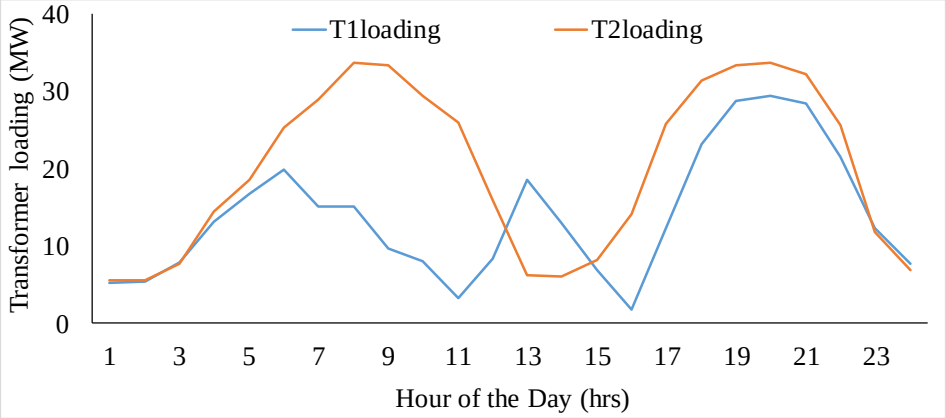

Fig. 30 Variation of Transformer loadings for a typical Day (Case 2.1 and 2.2)

6.3.2 Comparison of Test Cases 2.3 and 2.4 with 2.1

In Case 2.3, switch S_3 (connected between bus B_4 and B_{11}) is closed without implementing the Q(V) droop control strategy in the PV inverter whereas in the Case 2.4, switch remains closed, but Q(V) droop control strategy is implemented. The voltages comparison for both cases (Case 2.3 and 2.4) are shown in Figs. 31 and 32 respectively. As compare to the Case 2.3 with Case 2.1 (all switches open and without Q(V) droop), it is observed that there is not significant change in the voltage profiles. It implies that connected buses B_4 and B_{11} through switch S_3 doesn't improve the voltage profiles however, in Case 2.4 (S_3 closed and Q(V) droop implemented) voltage profiles are significant improved as compare to the Case 2.1 and the maximum voltage is reduced to 1.04 p.u. from 1.09 p.u.

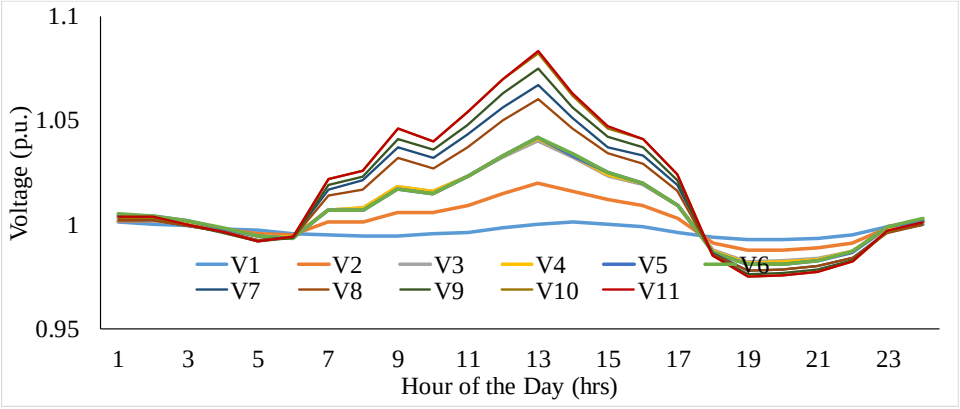

Fig. 31 Bus voltages at different bus terminals without Q(V) droop and S_3 closed (Case 2.3)

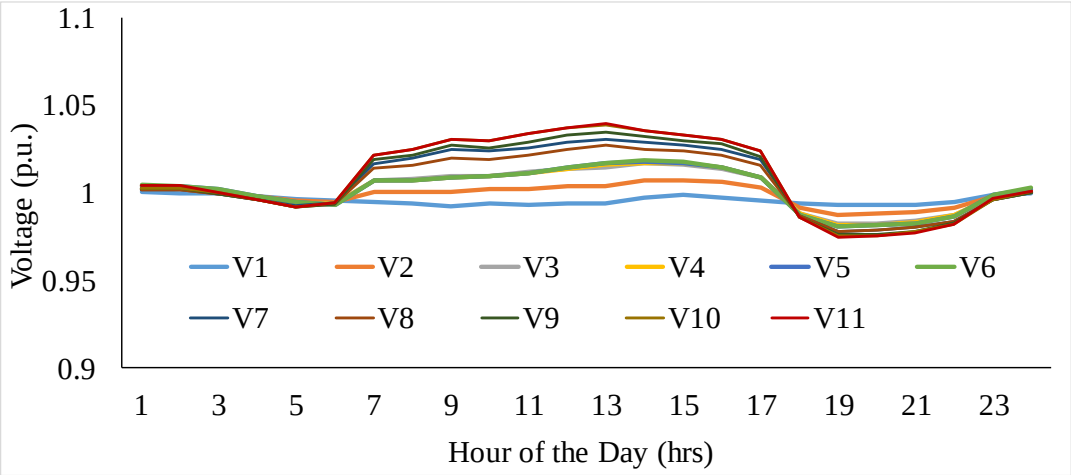

Fig. 32 Bus voltages at different bus terminals with Q(V) droop and S_3 closed (Case 2.4)

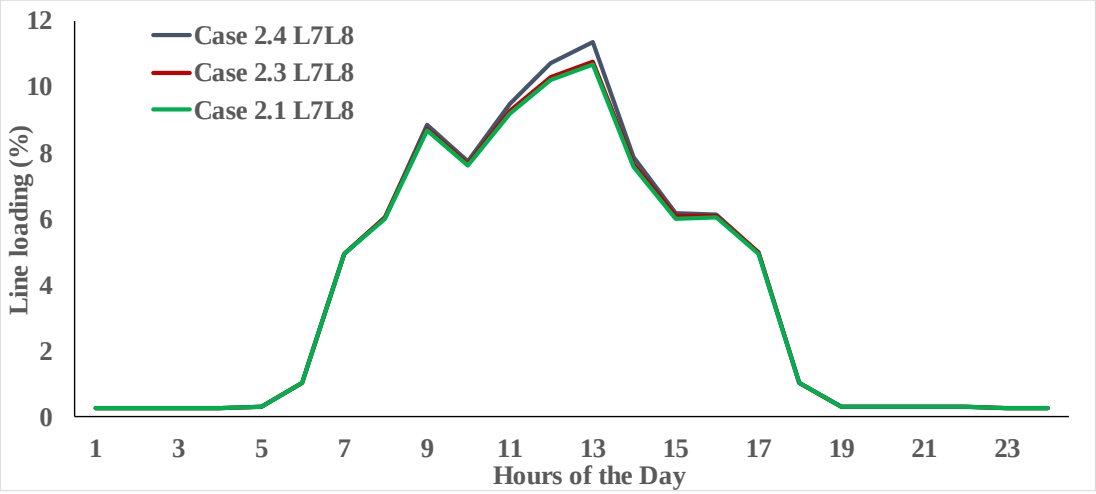

Fig. 33 Line loading of line L_3L_8 for Cases 2.3 and 2.4

A comparison of line loadings L_7L_8, for cases 2.1, 2.3 and 2.4 is shown in the Fig 33. It indicates that the by closing switch S_3, doesn't affect the line loading and for all three cases line (i.e. 2.1, 2.3 and 2.4) loading curve followed the same characteristics. There is no significant variation observed for transformer loading (TL_1 and TL_2) in Cases 2.3 and 2.4 as compare to the Case 2.1.

6.3.3 Comparison of Test Cases 2.5 and 2.6 with Case 2.1

In Case 2.5, switch S_2 (connected between bus B_6 and B_7) is closed without implementing the Q(V) droop control strategy in the PV inverter whereas in Case 2.6, switch S_2 remains closed, but Q(V) droop control strategy is implemented. The voltages comparison for both cases are shown in Figs. 34 and 35 respectively. While comparing the Case 2.5 with Case 2.1 (S_2 open and without Q(V) droop), it has been observed that there is not significant change in the voltage profiles. It implies that by closing S_2 doesn't change the voltage profiles however, Case 2.6 (S2 closed and Q(V) droop implemented) voltage profiles have been significant improved and the maximum voltage is reduced from 1.09 p.u. (Case 2.1) to 1.04 p.u.

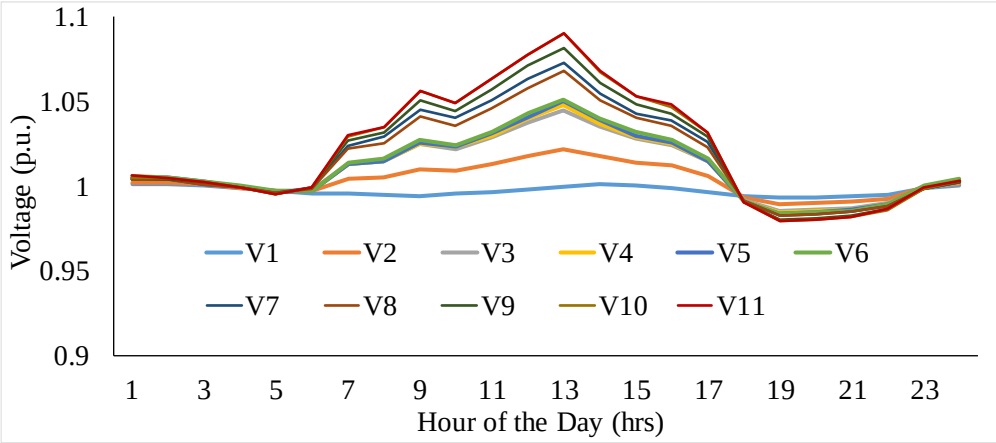

Fig. 34 Bus voltages at different bus terminals without Q(V) and S_2 closed (Case 2.5)

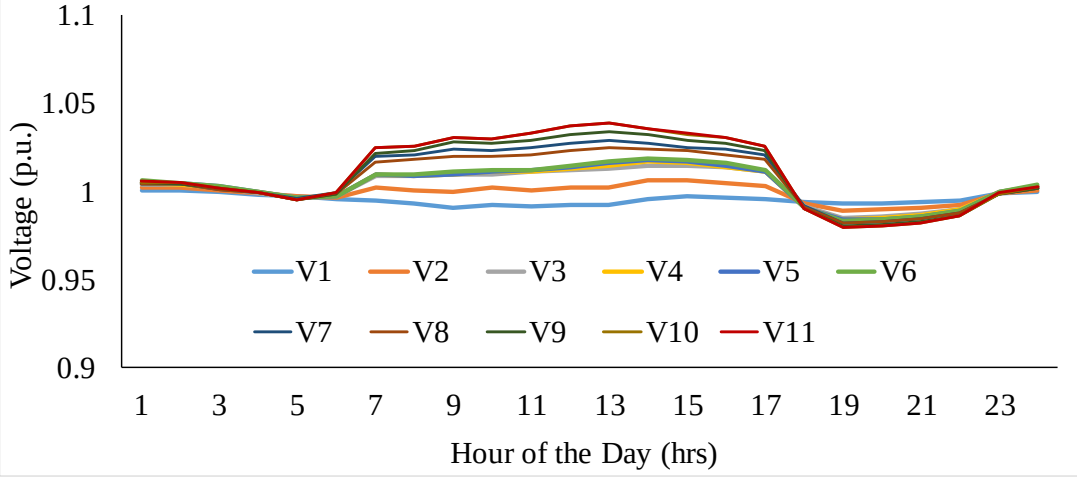

Fig. 35 Bus voltages at different bus terminals with Q(V) droop and S_1 closed (Case 2.6)

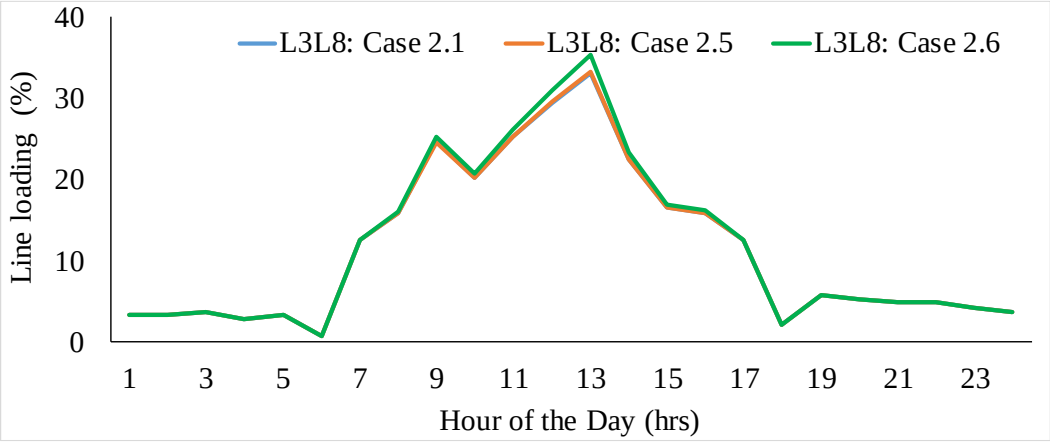

Fig. 36 Line loading of line L3L8 for Cases 2.1, 2.5 and 2.6

The line loading for L_3L_8 for Case 2.1, 2.5 & 2.6, is shown in Fig. 36. It has been observed that line loading followed similar characteristics in all the cases, and it implies that closing switch S_2 doesn't change the line loading too much. Also, there is no significant variation observed for transformer

loading (i.e. TL_1 and TL_2) in Case 2.5 and 2.6 as both feeders are not connected.

6.3.4 Comparison of Test Cases 2.7 and 2.8 with Case 2.1

In Case 2.7, switch S_1 (connected between bus B_8 and B_{14}) is closed without implementing the Q(V) droop control strategy in the PV inverter whereas in the Case 2.8, switch S_1 remains closed, but Q(V) droop control strategy is implemented. Switch S_1 is also important as it connects the both feeders together. The voltages comparison for both cases 2.7 and 2.8, are shown in Figs. 37 and 38 respectively. While comparing Case 2.7 with Case 2.1 (S_1 open and without Q(V) droop), it has been observed that the voltage profiles have been improved and maximum voltage is reduced to 1.05 p.u. from 1.09 p.u. (case 2.1). However, Case 2.8 (S_1 closed and Q(V) droop implemented) voltage profiles are further improved and the maximum voltage is reduced to 1.03 p.u.

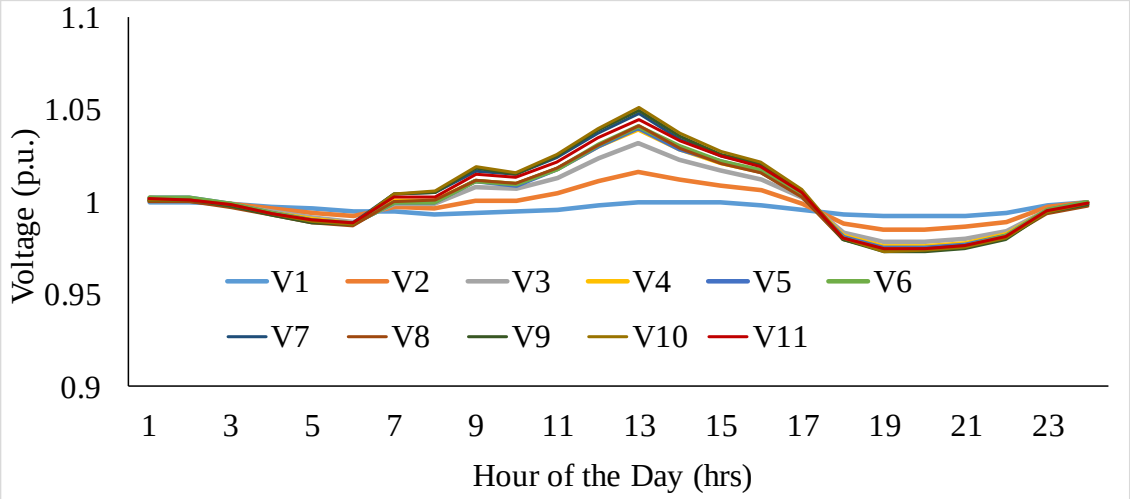

Fig. 37 Bus voltages at different bus terminals without Q(V) and S_1 closed (Case 2.7)

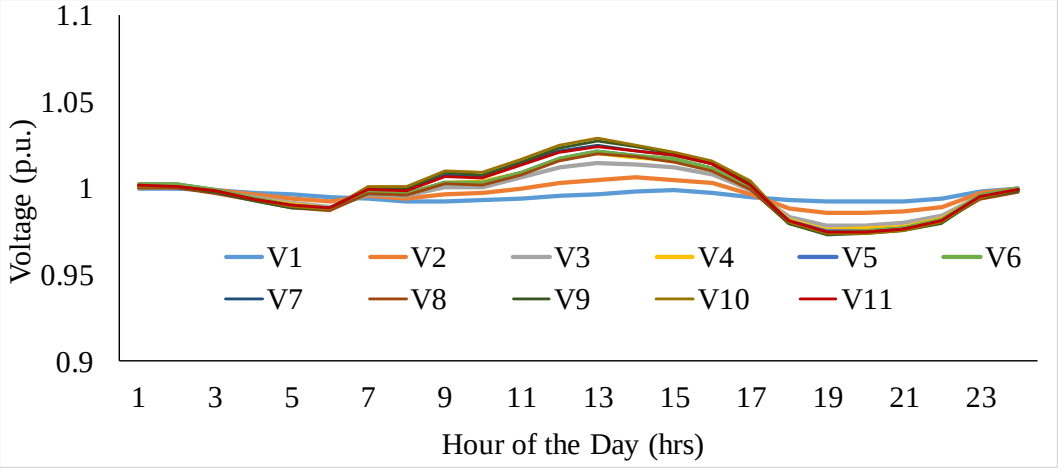

Fig. 38 Bus voltages at different bus terminals with Q(V) droop and S_1 closed (Case 2.8)

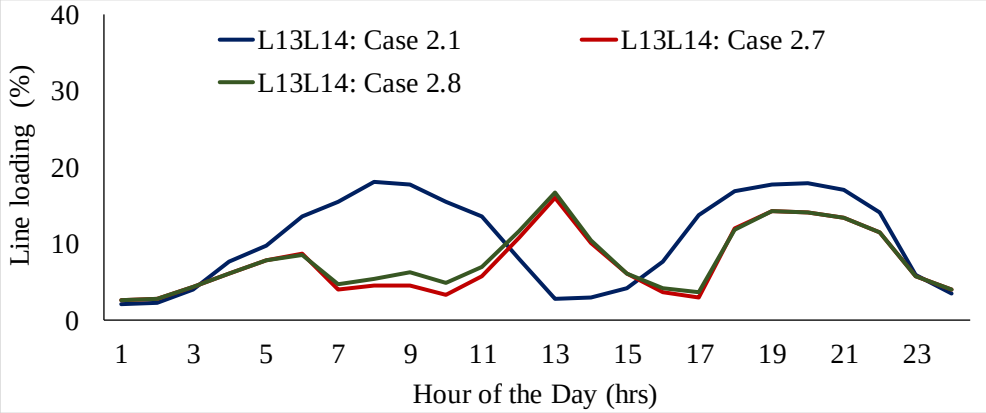

Fig. 39 Line loading of line $L_{13}L_{14}$ for Case 2.1, 2.7 and 2.8

The loading of the lines $L_{12}L_{13}$ and $L_{13}L_{14}$ are almost same therefore a comparison of only line loading $L_{13}L_{14}$ for the Case 2.1, Case 2.7 and Case 2.8 are considered for analysis purpose and shown in the Fig. 39. It has been observed from the Fig. 39 that loading of line $L_{13}L_{14}$ follows the characteristics for the Case 2.7 and 2.8 whereas it is different for Case 2.1. The maximum line loading for the Case 2.1 is observed during the peak demand's hours (i.e. 08:00 hours to 09:00 hours and 20:00 hours to 21:00 hours) and it is 18% however, in the Case 2.7 and 2.8, the maximum line loading is shifted to the peak sunshine hours (i.e.13:00 hours) and its value for Cases 2.7 and 2.8 are 16% and 17% respectively.

The loading of transformer TL_1 for the Cases 2.1, 2.7 and 2.8, are shown in the Fig. 40. While connected both feeders together, transformers loading are also changed for the Case 2.7 and 2.8 as compare to the Case 2.1. The maximum transformer loading of TL_1 of Case 2.1, during the daytime (i.e. 08:00 hours to 09:00 hours) peak load demand is increased from 15% (Case 2.1) to 20% (Cases 2.7 and 2.8) however maximum transformer loading of TL_1 of Case 2.1, during the night-time (20:00 hours to 21:00 hours) peak load demand only increased by 1% for (Cases 2.7 and 2.8). The transformer loading TL_1, during the peak sunshine hours (i.e. 13:00 hours) is decreased from 19% (Case 2.1) to 11% (Case 2.7) and 10% (Case 2.8) respectively.

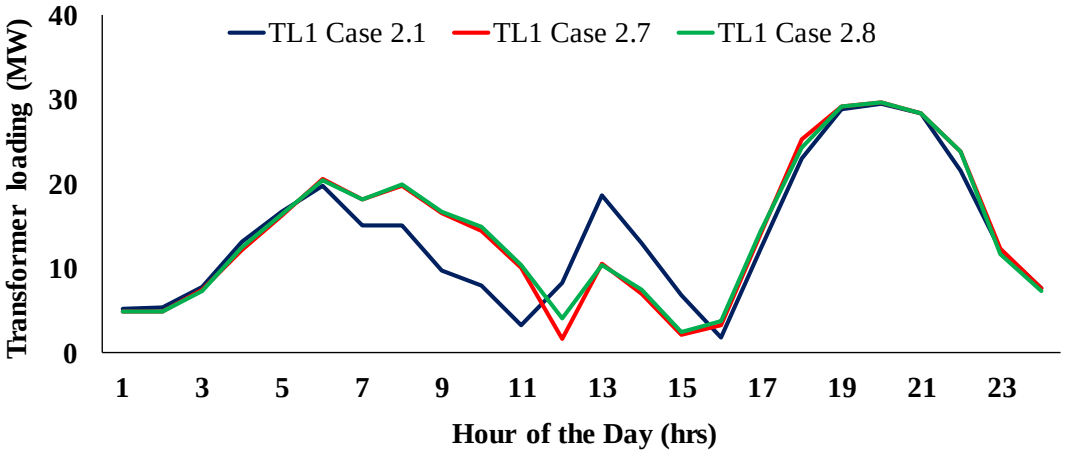

Fig. 40 Loading of Transformer TL_1 for Cases 2.1, 2.7 and 2.8

The loading of transformer TL_2 for the Cases 2.1, 2.7 and 2.8, are shown in the Fig. 41. The maximum transformer loading of TL_2 of Case 2.1, during the daytime (i.e. 08:00 hours to 09:00 hours) peak load demand is decreased from 34% (Case 2.1) to 27% (Cases 2.7 and 2.8) however, maximum transformer loading of TL_2 of Case 2.1, during the night-time (20:00 hours to 21:00 hours) peak load demand only decreased by 2% for (Cases 2.7 and 2.8). The transformer loading TL_2, during the

peak sunshine hours (i.e. 13:00 hours) is decreased from 6% (Case 2.1) to 2% (Case 2.7) and to 4% (Case 2.8). It has been observed that by connecting both feeder through Switch S_1, average transformer loading TL_2 reduced by 3%.

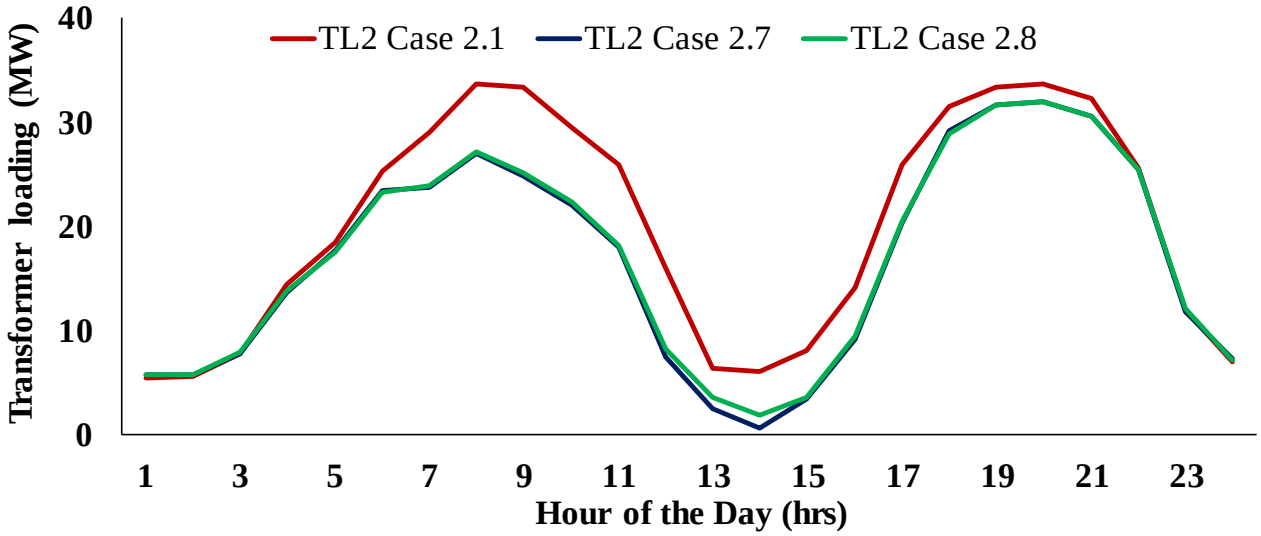

Fig. 41 Loading of Transformer TL_2 for Cases 2.1, 2.7 and 2.8

7 Conclusion

This work investigated voltage rise problem due to high PV penetration into the MV distribution network. In the first experiment, the CIGRE MV network is tested in the real time digital simulator and the Q(V) droop control strategy is implemented. It has been observed that appropriately implementing the Q(V) droop control strategy with the MV network, significantly improved the voltage profile. In the second experiment (PHIL method), a real hardware (i.e. grid tied PV inverter) is integrated in the MV network and the impact of PV penetration with and without Q(V) droop control strategies was tested and analysed. It also analysed the impact of different grid topologies and their impact on bus voltages, line loading and transformer loadings. It has been analysed that connecting both feeders through switch S_1, makes significant improvement in the voltage profiles within the MV network, however in the other grid topologies when switches S_2 and S_3 are closed, the voltage profiles are not much improved. It is also observed that by closing switch S_1 and connecting both feeders together, may be useful for balancing the transformer loadings of TL_1 and TL_2.

9 Dissemination Planning

Based on the results obtained from the experiment work, a research paper is being prepared for international conference or DBH approved/ peer reviewed journals. The article will be focused on the high PV penetration impact into the distribution network and role of droop control strategy to address the voltage rise issues.

10 Acknowledgement

The user is very much thankful to ERIGrid H2020 Research Infrastructure Project consortium for the transnational access opportunity to one of its testing and simulation facilities at SmartRUE Electric Energy Systems (EES) laboratory at the Institute of Communication and Computer Systems -National Technical University of Athens (ICCS-NTUA) and to the exceptional and friendly team for their assistance in the entire simulation and Power Hardware in-the-loop experiments.

11 References

[1] L.E. Weldemariam, V. Cuk, J.F.G. Cobben, ‘Impact of voltage dips monitored in the MV networks on aggregated customers’, Electric Power Systems Research, vol. 149, pp. 146-155, 2017.
[2] M. Karimi, H. Mokhlis, K. Naidu, S. Uddin, A.H.A. Bakar, ‘Photovoltaic penetration issues and impacts in distribution network – A review’, Renewable and Sustainable Energy Reviews, vol. 53, pp. 594-605, 2016.
[3] H. Ruf, M. Schroedter-Homscheidt, G. Heilscher, H.G. Beyer, ‘Quantifying residential PV feed-in power in low voltage grids based on satellite-derived irradiance data with application to power flow calculations’, Solar Energy, vol. 135, pp. 692-702, 2016.
[4] M. Böttiger, M. Paulitschke, T. Bocklisch, ‘Innovative reactive energy management for a photovoltaic battery system, Energy Procedia, vol. 99, pp. 341-349, 2016.
[5] ‘India’s Intended Nationally Determined Contribution’, UNFCC Report, pp. 1-38, 2015. [6] A Working report of IRENA, ‘Renewable Energy Prospects for India’, 2017.
[7] A.N. Azmi, I.N Dahlberg M.L Kolhe, A.G Imenes, Impact of Increasing Penetration of Photovoltaic Systems on Distribution Feeders. IEEE International Conference on Smart Grid and Clean Energy Technologies (ICSGCE), Offenburg, Germany, pp. 70 –74, 2015.
[8] A.N. Azmi, ‘Grid Interaction Performance Evaluation of BIPV and Analysis with Energy Storage on Distributed Network Power Management’, Ph.D. Thesis, University of Agder, Norway, March 2017.
[9] A report ‘EcoGrid EU Project’, Design to Implementation A large scale demonstration of a real-time marketplace for Distributed Energy Resources https://www.sintef.no/en/projects/-ecogrid-eu/
[10] A case study of Graciosa Adios Diesel-Ahoy Storage Microgrid and Island Energy Storage Solutions https://www.younicos.com/wp-content/uploads/2016/09/Younicos_-Microgrid_Solutions_EU.pdf
[11] A.N. Azmi, M.L Kolhe, A.G Imenes, ‘Technical and Economic Analysis for a Residential Grid Connected PV System with Possibilities of Different Battery Energy Storage Capacities (Case Study: Southern Norway)’, 4th International Workshop on Integration of Solar Power into Power Systems, Berlin, Energynautics GmbH. pp: 486 – 49, 2014.
[12] H. Samet, ‘Evaluation of digital metering methods used in protection and reactive power compensation of micro-grids’, Renewable and Sustainable Energy Reviews, vol. 62, pp. 260-279, 2016.
[13] L.B.G. Campanhol; S.A. Oliveira da Silva; A. Albano de Oliveira; V.D. Bacon, ‘Single-Stage Three-Phase Grid-Tied PV System With Universal Filtering Capability Applied to DG Systems and AC Microgrids’, IEEE Transactions on Power Electronics, vol. 32, issue 12, pp. 9131 – 9142, 2017.
[14] P.K.C. Wong; A. Kalam; R. Barr, ‘Modelling and analysis of practical options to improve the hosting capacity of low voltage networks for embedded photo-voltaic generation’, IET Renewable Power Generation, vol. 11, issue 5, pp. 625 – 632, 2017
[15] M. Elsied, A. Oukaour, T. Youssef, H. Gualous, O. Mohammed, ‘An advanced real time energy management system for microgrids’, Energy, vol. 114, pp. 742-752, 2016.
[16] Amelang, Sören, ‘The reform of the Renewable Energy Act: Germany's energy transition revamp stirs controversy over speed, participation’. Clean Energy Wire (CLEW), Berlin, Germany, 2016.
[17] M. Katsanevakis, R.A. Stewart, J. Lu, ‘Energy storage system utilization to increase photovoltaic penetration in low voltage distribution feeders’, Journal of Energy Storage, pp. 1-19, 2017.
[18] N. Martín-Chivelet, D. Montero-Gómez, ‘Optimizing photovoltaic self-consumption in office buildings’, Energy and Buildings, vol. 150, pp. 71-80, 2017.
[19] F. Marra, G. Yang, C. Træholt, J. Østergaard, E. Larsen, ‘A Decentralized Storage Strategy for Residential Feeders with Photovoltaics’, IEEE Transaction on Smart Grid, vol. 5, issue 2, pp. 974-981, Mar 2014.
[20] Benchmark Systems for Network Integration of Renewable and Distributed Energy Resources: 2014, ISBN: 978-285-873-270-8:
[21] M. Maniatopoulos, D. Lagos, P. Kotsampopoulos and N. Hatziargyriou, "Combined control and power hardware in-the-loop simulation for testing smart grid control algorithms," in IET Generation, Transmission & Distribution, vol. 11, no. 12, pp. 3009-3018, 24 8 2017.